

# Testing atomic wave functions in the nuclear vicinity: the hyperfine structure with empirically-deduced nuclear and quantum electrodynamic effects

J. S. M. Ginges<sup>1</sup> and A. V. Volotka<sup>2</sup>

<sup>1</sup>*Centre for Engineered Quantum Systems, School of Physics,  
The University of Sydney, Sydney NSW 2006, Australia*

<sup>2</sup>*Helmholtz-Institut Jena, Fröbelstieg 3, D-07743 Jena, Germany*  
(Dated: April 24, 2022)

In this Letter we propose a method for correcting atomic calculations of the hyperfine structure by accounting for the actual nuclear magnetic moment, nuclear magnetization distribution, and quantum electrodynamic (QED) radiative corrections through the use of measurements of the hyperfine structure for high states. The idea is based on the realization that the simple scaling  $\nu_{ns} = \mu/\mu_N \nu_{ns}^{\text{MB}} (1 + \alpha/\pi F^{\text{BW}} + \alpha/\pi F^{\text{QED}})$  is valid to high accuracy for all  $ns$  states, where  $\nu_{ns}$  is the total hyperfine splitting,  $\nu_{ns}^{\text{MB}}$  is the many-body atomic calculation of the hyperfine splitting for  $\mu = \mu_N$  and point-nucleus magnetization,  $\mu/\mu_N$  is the nuclear magnetic moment, and  $F^{\text{BW}}$ ,  $F^{\text{QED}}$  are the relative Bohr-Weisskopf and QED radiative corrections. When all effects are properly accounted for, the experimental value  $\nu_{ns}^{\text{exp}} = \nu_{ns}$ . The ratio  $\nu_{n's}^{\text{exp}}/\nu_{n's}^{\text{MB}}$  for higher states, where the accuracy for  $\nu_{n's}^{\text{MB}}$  is significantly better, is used to correct the theory value  $\nu_{ns}^{\text{MB}}$  for the lower states,  $\nu_{ns}^{\text{MB}} \left( \nu_{n's}^{\text{exp}}/\nu_{n's}^{\text{MB}} \right)$ , where the principal quantum number  $n < n'$ . The method is applied to published values for Cs and Fr [Gomez *et al.*, PRL **100**, 172502 (2008)], revealing the deviation of atomic many-body theory from experiment unencumbered by the uncertainties from nuclear physics and from the neglect of QED radiative corrections. This new ability to probe the electronic wave functions with sensitivity to the electron correlations has implications for the analysis of parity violation measurements and opens the way for significantly improved atomic parity violation calculations. This ratio method may also be used for high-accuracy predictions.

Studies of atomic parity violation provide important low-energy tests of the standard model of particle physics. The largest effect in atoms arises from the nuclear weak charge which depends on a unique combination of fundamental coupling constants. This makes atomic parity violation measurements uniquely sensitive to certain types of new physics, complementing searches for new physics performed at high energies [1–3].

Extraction of the nuclear weak charge from atomic measurements requires high-precision atomic calculations (see, e.g., the review [4]). For example, for Cs  $6S_{1/2} - 7S_{1/2}$ , this corresponds to evaluation of the second-order expression

$$E_{\text{PV}} = \sum_n \frac{\langle 7S_{1/2} | D | nP_{1/2} \rangle \langle nP_{1/2} | H_{\text{PV}} | 6S_{1/2} \rangle}{E_{6S_{1/2}} - E_{nP_{1/2}}} + \sum_n \frac{\langle 7S_{1/2} | H_{\text{PV}} | nP_{1/2} \rangle \langle nP_{1/2} | D | 6S_{1/2} \rangle}{E_{7S_{1/2}} - E_{nP_{1/2}}}, \quad (1)$$

where  $6S_{1/2}$ ,  $7S_{1/2}$ ,  $nP_{1/2}$  are many-body atomic states,  $\mathbf{D} = \sum_i |e| \mathbf{r}_i$  is the electric dipole operator acting over the  $i$  electrons of the atom,  $H_{\text{PV}}$  is the weak operator that is localized on the nucleus, and  $E$  are atomic binding energies. To gauge the accuracy of these calculations, comparison of theoretical and experimental determinations of electric dipole transition amplitudes, energy intervals, and hyperfine structure intervals is made [5, 6]. The hyperfine structure is sensitive to the atomic wave functions in the nuclear region, and it is the hyperfine structure for which the largest deviations are seen.

The atoms/ions of interest for atomic parity violation measurements include the alkali-metal atoms and alkali-metal-like ions Cs [7], Fr [8–10], Ba<sup>+</sup> [11, 12], and Ra<sup>+</sup> [13]. The highest precision in atomic parity violation studies has been reached for <sup>133</sup>Cs, the measurement accurate to 0.35% [14] and calculations accurate to within 0.5% [5, 6, 15, 16]. The atomic theory uncertainty is considered to be a limiting factor in the interpretation of future measurements.

In this Letter, we pave the way for significantly improved understanding of the electronic wave functions in the nuclear region. We propose a method for empirically correcting the unknown or neglected nuclear properties and quantum electrodynamic (QED) radiative corrections in hyperfine structure calculations by exploiting the scaling of different effects for higher states. The method is applied to published data for <sup>133</sup>Cs and <sup>210</sup>Fr [17], revealing remarkably better agreement between theory and experiment.

Beyond the uncertainties associated with many-electron correlations in the atomic theory evaluation of the hyperfine structure, there are several other sources of uncertainty related to assumed values of (i) the nuclear magnetic moment, (ii) the finite-magnetization distribution of the nucleus, and (iii) QED radiative corrections (or their neglect). The size of the error associated with each of these may be several 0.1%, or even  $\approx 1\%$ , for the systems of interest for parity violation studies. Controlling these errors is crucial if  $\approx 0.1\%$  tests of the electron correlation calculations in the nuclear vicinity are to be

made.

Indeed, (i) in the comparison between theory and experiment for the hyperfine structure, a value for the nuclear magnetic moment is assumed. However, for the Fr isotopes, these are not known to better than 1-2% [17, 18]. (ii) An assumed magnetization distribution is used in atomic calculations, the most routinely-used being the uniformly magnetized sphere. There is data, however, for the hyperfine structure for the neutron-deficient isotopes of Fr [19, 20] that supports the validity of the single-particle model for that system. In our recent work [21], we demonstrated that using the single-particle model gives a result for  $^{211}\text{Fr}$  that differs by nearly 1.5% from that found using the sphere; for  $^{133}\text{Cs}$  this difference is 0.5%. (iii) Rigorous calculations are required for reliable determination of QED radiative corrections to the hyperfine structure. Such calculations at one-loop level have been performed for the alkali-metal atoms [22, 23] and only recently for alkali-metal-like ions  $\text{Ba}^+$  and  $\text{Ra}^+$  [23], with contributions entering at around 0.5% for Cs,  $\text{Ba}^+$ , Fr,  $\text{Ra}^+$ . Overwhelmingly, these effects have been neglected (or very crudely estimated) in theoretical determinations of the hyperfine structure.

We note that the uncertainty associated with the nuclear magnetization distribution also poses a problem in the area of QED tests in few-electron highly-charged ions. That problem is addressed by constructing a difference between hyperfine intervals of the ion in question and the hydrogen-like ion that cancels the effect [24].

The magnetic hyperfine interaction is given by

$$h_{\text{hfs}} = c\boldsymbol{\alpha} \cdot \mathbf{A} = \frac{1}{c} \frac{\boldsymbol{\mu} \cdot (\mathbf{r} \times \boldsymbol{\alpha})}{r^3} F(r), \quad (2)$$

where  $\boldsymbol{\mu} = \mu\mathbf{I}/I$  is the nuclear magnetic moment and  $I$  is the nuclear spin,  $\boldsymbol{\alpha} = \gamma_0\boldsymbol{\gamma}$  is the Dirac matrix, and  $F(r)$  describes the magnetization distribution. We use atomic units ( $|e| = m = \hbar = 4\pi\epsilon_0 = 1$ ,  $c = 1/\alpha$ ).  $F(r) = 1$  corresponds to the case of point-nucleus magnetization. For a finite-nucleus magnetization distribution, the value  $F(r) - 1$  differs from zero within the nucleus,  $r \leq r_n$ . Account of finite-nucleus magnetization gives a correction to the (point-magnetization) hyperfine structure – the Bohr-Weisskopf (BW) effect [25].

For  $^2S_{1/2}$  states in the atom, the hyperfine interaction splits the level into states described by the total angular momenta  $F = I \pm 1/2$ . The interval between hyperfine levels in the zeroth-order approximation (lowest-order in the atomic potential and for point-nuclear magnetization) is

$$\nu^{(0)} = \frac{2}{3} \frac{\alpha^2}{m_p} g_I (2I + 1) \int_0^\infty dr f(r)g(r)/r^2, \quad (3)$$

where  $m_p$  is the proton mass,  $g_I = \mu/(\mu_N I)$  is the nuclear g-factor, and  $f(r)$  and  $g(r)$  are the upper and lower radial components of the relativistic wave functions  $\varphi$

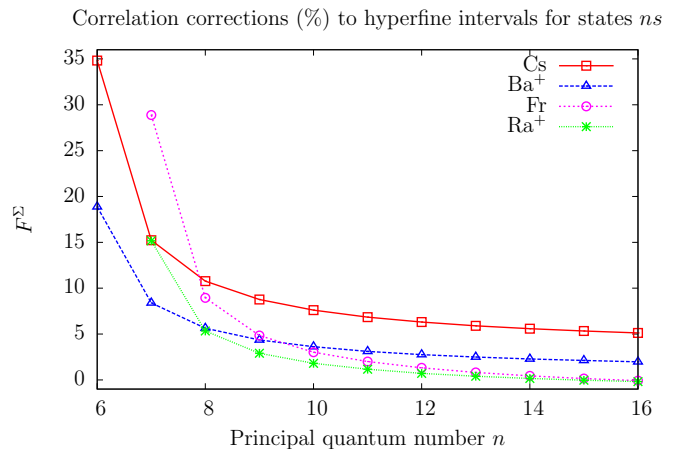


FIG. 1. Relative correlation corrections  $F^\Sigma$  to the hyperfine structure (in %) for Cs,  $\text{Ba}^+$ , Fr,  $\text{Ra}^+$ . This corresponds to evaluation of  $\langle \varphi_{\text{Br}} | h_{\text{hfs}} + \delta V_{\text{hfs}} | \varphi_{\text{Br}} \rangle - \langle \varphi | h_{\text{hfs}} + \delta V_{\text{hfs}} | \varphi \rangle$  relative to  $\langle \varphi | h_{\text{hfs}} + \delta V_{\text{hfs}} | \varphi \rangle$

that satisfy the Dirac equation

$$(c\boldsymbol{\alpha} \cdot \mathbf{p} + (\beta - 1)c^2 + V_{\text{nuc}}(r) + V_{\text{el}})\varphi = \epsilon\varphi. \quad (4)$$

In our many-body calculations for the hyperfine interval, we use the Hartree-Fock potential as our starting potential,  $V_{\text{el}} = V_{\text{HF}}$ . For calculations of the QED radiative corrections, we use two different potentials for  $V_{\text{el}}$ , core-Hartree  $V_{\text{CH}}$  (corresponding to neglecting the exchange potential in Hartree-Fock) and Kohn-Sham  $V_{\text{KS}}$  [26]. Finite nuclear charge distribution is included in the determination of the wave functions, with  $V_{\text{nuc}}$  corresponding to a 2-parameter Fermi distribution.

We parameterize the total hyperfine interval for the state  $ns$ , where  $n$  is the principal quantum number, as

$$\nu_{ns} = \frac{\mu}{\mu_N} \nu_{ns}^{\text{MB}} \left( 1 + \frac{\alpha}{\pi} F^{\text{BW}} + \frac{\alpha}{\pi} F^{\text{QED}} \right), \quad (5)$$

where we explicitly show the dependence on  $\mu$ , and the many-body value of the hyperfine interval  $\nu_{ns}^{\text{MB}}$  for state  $ns$  is found with  $\mu = \mu_N$  and point-nucleus magnetization,  $F^{\text{BW}}$  is the relative finite-magnetization correction to the hyperfine interval, and  $F^{\text{QED}}$  is the relative quantum electrodynamic radiative correction. In the following, we will consider how the relative correlation corrections  $F^\Sigma$  and relative Bohr-Weisskopf  $F^{\text{BW}}$  and quantum electrodynamic  $F^{\text{QED}}$  corrections scale for higher principal quantum numbers  $n'$ .

Our many-body calculations are carried out using the correlation potential approach [27]. A non-local, energy-dependent correlation potential  $\Sigma(\mathbf{r}, \mathbf{r}', \epsilon)$  is constructed such that, in lowest order, the average value of this potential coincides with the second-order correlation correction to the energy. We use the Feynman diagram technique to include electron-electron screening and the hole-particle

interaction to all orders in the Coulomb interaction [28]. This potential is added to the relativistic Hartree-Fock equation (4), with  $V_{\text{HF}} \rightarrow V_{\text{HF}} + \Sigma^{(\infty)}$ , and correlation-corrected (Brueckner) energies  $\epsilon_{\text{Br}}$  and orbitals  $\varphi_{\text{Br}}$  are obtained.

The dominant part of the external-field correlation corrections – the core polarization – is included using the random-phase approximation with exchange (RPA). From this we get a correction to the hyperfine operator which corresponds to a hyperfine-modified Hartree-Fock potential,  $h_{\text{hfs}} + \delta V_{\text{hfs}}$  [27]. Inclusion of the correlation potential and RPA corrections corresponds to evaluation of the matrix element  $\langle \varphi_{\text{Br}} | h_{\text{hfs}} + \delta V_{\text{hfs}} | \varphi_{\text{Br}} \rangle$ .

In Fig. 1 we plot the relative correlation corrections for  $ns$  states from the ground state to principal quantum number  $n = 16$  for alkali-metal atoms and alkali-metal-like ions of interest for parity violation studies, Cs, Fr, Ba<sup>+</sup>, Ra<sup>+</sup>. These corrections correspond to the difference  $\langle \varphi_{\text{Br}} | h_{\text{hfs}} + \delta V_{\text{hfs}} | \varphi_{\text{Br}} \rangle - \langle \varphi | h_{\text{hfs}} + \delta V_{\text{hfs}} | \varphi \rangle$  relative to  $\langle \varphi | h_{\text{hfs}} + \delta V_{\text{hfs}} | \varphi \rangle$  which we denote by  $F^\Sigma$ . Since most of the uncertainty in many-body calculations is associated with evaluation of the correlations, the smaller the relative size of the correlations  $F^\Sigma$ , the smaller the error in the many-body calculations. We observe a sharp drop in the relative size of the correlations from  $ns$  to  $(n+1)s$ , and the corrections continue to decrease with higher  $n$ . We may therefore expect that the many-body evaluation of the hyperfine structure is of significantly higher accuracy for  $\epsilon_{n's}^{\text{MB}}$  compared to the ground or lower level  $\epsilon_{ns}^{\text{MB}}$ , where  $n' > n$  and particularly for  $n' \gg n$ .

We have studied the scaling of the Bohr-Weisskopf effect in two very different magnetization models: (i) the uniform spherical distribution, where  $F(r) = (r/r_n)^3$ , and (ii) the nuclear single-particle model, with spin nucleon  $g$ -factors found from measured nuclear magnetic moments. We refer the reader to, e.g., Ref. [29] for the single-particle model expressions for  $F(r)$ , derived in Refs. [25, 30–32]. We performed calculations for <sup>133</sup>Cs with  $5 \times 10^4$  grid points. At the Hartree-Fock level, we obtained a result  $F^{\text{BW}} = -3.069$  in the spherical model and  $F^{\text{BW}} = -0.8940$  in the single-particle model. We have checked the robustness of these results at different levels of many-body approximation, with core polarization included, with core polarization and the correlation potential, and with Breit. Inclusion of core polarization gave the largest correction, changing the result for  $F^{\text{BW}}$  by only 0.4%. The results for  $F^{\text{BW}}$  change only by about 0.1% at most for different principal quantum numbers,  $n = 6 - 10$ .

We have calculated the QED radiative corrections for <sup>133</sup>Cs over  $n = 6 - 10$ . Rigorous calculations of the one-loop self-energy and vacuum polarization corrections were performed using the extended Furry picture with the core-Hartree (CH) potential and the Kohn-Sham (KS) potential generated for the ground state. Expressions were derived using the two-time Green's function

method [33]. Details of the method of evaluation may be found in Ref. [29]. In Table I we present our results. The correction changes relatively significantly from  $n = 6$  through to  $n = 10$  (20% for CH and 17% for KS), however a difference of 20% in  $F^{\text{QED}}$  gives a change of only 0.05% in  $(\alpha/\pi)F^{\text{QED}}$ .

TABLE I. Relative QED radiative corrections  $F^{\text{QED}}$  to hyperfine intervals for  $ns$  states of <sup>133</sup>Cs found in core-Hartree and Kohn-Sham potentials,  $V_{\text{CH}}$  and  $V_{\text{KS}}$ .

	$F^{\text{QED}}$				
	6s	7s	8s	9s	10s
$V_{\text{CH}}$	-1.64	-1.49	-1.44	-1.39	-1.31
$V_{\text{KS}}$	-1.91	-1.77	-1.71	-1.65	-1.59

Without loss of generality, we may write for the higher states

$$\nu_{n's} = \frac{\mu}{\mu_N} \nu_{n's}^{\text{MB}} \left( 1 + \frac{\alpha}{\pi} F^{\text{BW}} + \delta^{\text{BW}} + \frac{\alpha}{\pi} F^{\text{QED}} + \delta^{\text{QED}} \right), \quad (6)$$

where  $\delta^{\text{BW}} = \alpha/\pi (F^{\text{BW}'} - F^{\text{BW}})$  and  $\delta^{\text{QED}} = \alpha/\pi (F^{\text{QED}'} - F^{\text{QED}})$ . We have shown for Cs that comfortably  $\delta^{\text{BW}} \ll \delta^{\text{QED}} < 0.001$ . Therefore, we propose to write the hyperfine splitting for the higher states  $n's$  with the same scaling as for the lowest level in Eq. (5),

$$\nu_{n's} = \frac{\mu}{\mu_N} \nu_{n's}^{\text{MB}} \left( 1 + \frac{\alpha}{\pi} F^{\text{BW}} + \frac{\alpha}{\pi} F^{\text{QED}} \right). \quad (7)$$

The total hyperfine interval, when the “true” many-body, nuclear magnetic moment, finite magnetization, and QED effects are considered, coincides with the experimental value for the hyperfine interval,

$$\nu_{n's}^{\text{exp}} = \nu_{n's}. \quad (8)$$

Since the hyperfine interval for the high state  $n's$  may be calculated with significantly higher accuracy than for the lower level  $ns$ , the ratio

$$\nu_{n's}^{\text{exp}} / \nu_{n's}^{\text{MB}} \quad (9)$$

may be used for high-precision determination of the nuclear and QED parameters

$$\frac{\mu}{\mu_N} \left( 1 + \frac{\alpha}{\pi} F^{\text{BW}} + \frac{\alpha}{\pi} F^{\text{QED}} \right) \quad (10)$$

which may then be used to correct the theory values for the ground and lower states,

$$\nu_{ns} = \nu_{ns}^{\text{MB}} (\nu_{n's}^{\text{exp}} / \nu_{n's}^{\text{MB}}). \quad (11)$$

Before we apply this method, let's consider for a moment the ratio  $\nu_{ns}^{\text{MB}} / \nu_{n's}^{\text{MB}}$  in Eq. (11). The many-body value for the hyperfine interval may be approximately expressed as

$$\nu_{ns}^{\text{MB}} \approx \nu^{\text{HF}} (1 + F^{\delta V}) (1 + F^\Sigma), \quad (12)$$

TABLE II. Calculations of the magnetic hyperfine A constants for  $^{133}\text{Cs}$  and  $^{210}\text{Fr}$  from Ref. [17]. Raw values  $A_{n's}$  and percentage deviations from experiment are presented in the first two columns of results, corrected many-body values using ratios from  $(n+2)s$  and  $(n+1)s$  states are presented in the following columns alongside their percentage deviations from experiment, and measured values and references are presented in the final two columns. In the table we use  $n$  to denote the ground state principal quantum number and  $n'$  to denote arbitrary principal quantum number. Units: MHz.

Atom	State	$A_{n's}$ [17]	% dev.	$(A_{(n+2)s}^{\text{exp}}/A_{(n+2)s})A_{n's}$	% dev.	$(A_{(n+1)s}^{\text{exp}}/A_{(n+1)s})A_{n's}$	% dev.	$A_{n's}^{\text{exp}}$	Ref.
$^{133}\text{Cs}$	6s	2276	-1.0	2300	0.1	2301	0.1	2298.157	[34]
	7s	540.0	-1.0	545.8	0.0			545.818(16)	[35]
	8s	216.8	-1.1					219.125(4)	[36]
$^{210}\text{Fr}$	7s	7277	1.1	7247	0.7	7249	0.7	7195.1(4)	[37]
	8s	1584	0.4	1578	0.0			1577.8(11)	[38]
	9s	624.8	0.4					622.25(36)	[17]

where  $\nu^{\text{HF}}$  is the hyperfine interval found in the relativistic Hartree-Fock approximation and  $F^{\delta V}$ ,  $F^{\Sigma}$  are the relative RPA and correlation corrections. The RPA correction is essentially the same for all principal quantum numbers – for Cs,  $F^{\delta V} \approx 0.2$  – and it cancels in the ratio Eq. (11). It means that the ratio method is largely insensitive to the theoretical account of the core polarization, with this correction included empirically through  $\nu_{n's}^{\text{exp}}$ .

The atomic theory error, however, is mainly associated with the evaluation of the electron-electron correlations, most of which may be represented by a correlation potential  $\Sigma$ . For the correlation potential, and smaller correlation corrections, the relative correction is not the same for different  $n$ , and we have

$$\nu_{ns}^{\text{MB}}/\nu_{n's}^{\text{MB}} \approx \nu_{ns}^{\text{HF}}/\nu_{n's}^{\text{HF}} (1 + F_{ns}^{\Sigma} - F_{n's}^{\Sigma}). \quad (13)$$

The ratio therefore depends on the difference in the relative correlation corrections between states  $ns$  and  $n's$ ,  $F_{ns}^{\Sigma} - F_{n's}^{\Sigma}$ . If we are interested in preserving the dependence on the theoretical account of the electron correlations (i.e., we want to test the accuracy of atomic calculations), then this difference should be as large as possible,  $F_{ns}^{\Sigma} \gg F_{n's}^{\Sigma}$ . The most suitable state to test is therefore the ground state, with the other state chosen to be as high as possible (see Fig. 1). On the other hand, for the case where  $F_{ns}^{\Sigma} - F_{n's}^{\Sigma} \approx 0$  (both states with high principal quantum number), the dependence on the theoretical account of the correlations is removed in the ratio, and we may perform high-precision predictions of the hyperfine structure.

We apply the ratio method to published values of Gomez *et al.* [17] where the lowest three levels for the hyperfine A constants for  $^{133}\text{Cs}$  and  $^{210}\text{Fr}$  have been calculated and for which high-precision measurements are available. The results are shown in Table II. In the first column are the raw values from Ref. [17], where a two-parameter Fermi distribution for the magnetization was used, where radiative corrections were neglected, and where the nuclear magnetic moment for  $^{210}\text{Fr}$  was taken to be  $\mu = 4.40\mu_N$  [18]. The deviation of these results

from experiment is shown in the next column, seen to be around -1% for  $^{133}\text{Cs}$  for all three states and for  $^{210}\text{Fr}$  the ground state deviation is 1.1% and 0.4% for the higher levels. The ratio determined from the high levels  $(n+2)s$  is applied to the lower  $(n+1)s$  and ground  $ns$  levels, giving the values for the hyperfine constants presented in the next column. The improvement in the agreement with experiment is remarkable. For  $^{210}\text{Fr}$ , there is exact agreement for the 8s state and a deviation of 0.7% for 7s, while for  $^{133}\text{Cs}$  the value for 7s agrees exactly with experiment and for 6s there is a deviation of only 0.1%. If we apply the ratio from the  $(n+1)s$  states, we obtain essentially the same results for the ground state hyperfine intervals as we did using the  $(n+2)s$  ratios. The coincidence of the results with rescaling from  $(n+1)$  and  $(n+2)$  lends support to the validity of the scaling and the high accuracy of calculations. Note that this procedure for testing the atomic theory is equivalent to comparing the theory ratio  $\nu_{ns}/\nu_{n's}$  or  $\nu_{ns}^{\text{MB}}/\nu_{n's}^{\text{MB}}$  with the empirical one  $\nu_{ns}^{\text{exp}}/\nu_{n's}^{\text{exp}}$ .

The value used for the nuclear magnetic moment for  $^{210}\text{Fr}$  in the raw data of Ref. [17] has an uncertainty of 2% [18, 39]. By using the proposed ratio method, Eq. (11), the physical value for the nuclear magnetic moment is included through the measured value of the high states, with the assumed theoretical value cancelling in the ratio of the theory values,  $\nu_{ns}/\nu_{n's} = \nu_{ns}^{\text{MB}}/\nu_{n's}^{\text{MB}}$ . Moreover, while the QED radiative corrections were not included in Ref. [17], it is clear that account of these corrections,  $[1 + (\alpha/\pi)F^{\text{BW}} + (\alpha/\pi)F^{\text{QED}}] \approx [1 + (\alpha/\pi)F^{\text{BW}}][1 + (\alpha/\pi)F^{\text{QED}}]$ , would be removed in the theory ratio and input from the measured value for high states. In the same way, the dependence on the chosen magnetization distribution is removed.

By correcting for the actual nuclear magnetic moments, actual magnetization distribution of the nucleus, and neglect of QED radiative corrections, it is seen that the many-body calculations of Gomez *et al.* [17] are of significantly higher accuracy than previously considered. With the ratio method we have proposed, the electron

wave functions for the low states may be probed reliably for the first time. The sensitivity to the electron correlations is best for the ground states, and a more reliable result may be obtained by using a ratio from higher states where  $F_{n's}^{\Sigma}$  is smaller.

For the excited states  $7s$  and  $8s$  for Cs and Fr, respectively, it is natural to expect higher accuracy in the calculations compared to those for the ground states. However, part of the dependence on electron correlations is removed and corrected empirically in the ratio (11) for the excited states, which explains to some degree the remarkable agreement of the ratio-corrected results with experiment. The deviation from experiment for the excited states gives a lower bound on the error of many-body calculations.

Using the data from Ref. [17], we again demonstrate the predictive power of the ratio (11). For  $^{133}\text{Cs } 8s$ , we obtain a “prediction” of 219.1 MHz using the data for  $7s$ , agreeing with the measured value 219.125(4) MHz [36]. For  $^{210}\text{Fr } 9s$ , we obtain 622.4 MHz from the data for  $8s$ , in agreement with the experimental value 622.25(36) MHz [17].

High-precision measurements of the hyperfine structure intervals for  $s$ -states of Rydberg levels would prove invaluable for correcting atomic calculations by means of the proposed ratio method.

J. Ginges is grateful to A. Doherty and S. Bartlett for useful discussions and to the Mainz Institute for Theoretical Physics (MITP) for hospitality and support over a two-week visit during the Low-Energy Probes of New Physics program. This work was supported by the Australian Research Council through the Centre of Excellence in Engineered Quantum Systems (EQuS), project number CE110001013.

- 
- [1] W. J. Marciano and J. L. Rosner, *Phys. Rev. Lett.* **65**, 2963 (1990).
- [2] V. Cirigliano and M. J. Ramsey-Musolf, *Prog. in Part. and Nucl. Phys.* **71**, 2 (2013).
- [3] J. Erler and S. Su, *Prog. in Part. and Nucl. Phys.* **71**, 119 (2013).
- [4] J. S. M. Ginges and V. V. Flambaum, *Phys. Rep.* **397**, 63 (2004).
- [5] V. A. Dzuba, V. V. Flambaum, and J. S. M. Ginges, *Phys. Rev. D* **66**, 076013 (2002).
- [6] S. G. Porsev, K. Beloy, and A. Derevianko, *Phys. Rev. Lett.* **102**, 181601 (2009).
- [7] J. Guéna, D. Chauvat, Ph. Jacquier, E. Jahier, M. Lintz, S. Sanguinetti, A. Wasan, M. A. Bouchiat, A. V. Papoyan, and D. Sarkisyan, *Phys. Rev. Lett.* **90**, 143001 (2003).
- [8] E. Gomez, L. A. Orozco, and G. D. Sprouse, *Rep. Prog. Phys.* **69**, 79 (2006).
- [9] E. Gomez, S. Aubin, R. Collister, J. A. Behr, G. Gwinner, L. A. Orozco, M. R. Pearson, M. Tandecki, D. Sheng, and J. Zhang, *J. Phys. Conf. Series* **387**, 012004 (2012).
- [10] M.-A. Bouchiat, *Phys. Rev. Lett.* **100**, 123003 (2008).
- [11] N. Fortson, *Phys. Rev. Lett.* **70**, 2383 (1993).
- [12] T. W. Koerber, M. Schacht, W. Nagourney and E. N. Fortson, *J. Phys. B* **36**, 637 (2003).
- [13] M. Nuñez Portela, E. A. Dijck, A. Mohanty, H. Bekker, J. E. van den Berg, G. S. Giri, S. Hoekstra, C. J. G. Onderwater, S. Schlessler, R. G. E. Timmermans, O. O. Versolato, L. Willmann, H. W. Wilschut, and K. Jungmann, *Appl. Phys. B* **114**, 173 (2014).
- [14] C. S. Wood, S. C. Bennett, D. Cho, B. P. Masterson, J. L. Roberts, C. E. Tanner, and C. E. Wieman, *Science* **275**, 1759 (1997).
- [15] V. V. Flambaum and J. S. M. Ginges, *Phys. Rev. A* **72**, 052115 (2005).
- [16] V. A. Dzuba, J. C. Berengut, V. V. Flambaum, and B. Roberts, *Phys. Rev. Lett.* **109**, 203003 (2012).
- [17] E. Gomez, S. Aubin, L. A. Orozco, G. D. Sprouse, E. Iskrenova-Tchoukova, and M. S. Safronova, *Phys. Rev. Lett.* **100**, 172502 (2008).
- [18] C. Ekström, L. Robertsson, and A. Rosén, *Phys. Scr.* **34**, 624 (1986).
- [19] J. S. Grossman, L. A. Orozco, M. R. Pearson, J. E. Sim-sarian, G. D. Sprouse, and W. Z. Zhao, *Phys. Rev. Lett.* **83**, 935 (1999).
- [20] J. Zhang, M. Tandecki, R. Collister, S. Aubin, J. A. Behr, E. Gomez, G. Gwinner, L. A. Orozco, M. R. Pearson, and G. D. Sprouse, *Phys. Rev. Lett.* **115**, 042501 (2015).
- [21] J. S. M. Ginges, A. V. Volotka, and S. Fritzsche, in preparation.
- [22] J. Sapirstein and K. T. Cheng, *Phys. Rev. A* **67**, 022512 (2003).
- [23] J. S. M. Ginges, A. V. Volotka, and S. Fritzsche, in preparation.
- [24] V. M. Shabaev, A. N. Artemyev, V. A. Yerokhin, O. M. Zherebtsov, and G. Soff, *Phys. Rev. Lett.* **86**, 3959 (2001).
- [25] A. Bohr and V. F. Weisskopf, *Phys. Rev.* **77**, 94 (1950).
- [26] W. Kohn and L. J. Sham, *Phys. Rev.* **140**, A1133 (1965).
- [27] V. A. Dzuba, V. V. Flambaum, P. G. Silvestrov, O. P. Sushkov, *J. Phys. B* **20**, 1399 (1987).
- [28] V. A. Dzuba, V. V. Flambaum, P. G. Silvestrov, O. P. Sushkov, *Phys. Lett. A* **131**, 461 (1988).
- [29] A. V. Volotka, D. A. Glazov, I. I. Tupitsyn, N. S. Oreshkina, G. Plunien, and V. M. Shabaev, *Phys. Rev. A* **78**, 062507 (2008).
- [30] M. Le Bellac, *Nucl. Phys.* **40**, 645 (1963).
- [31] V. M. Shabaev, *J. Phys. B* **27**, 5825 (1994).
- [32] V. M. Shabaev, M. Tomaselli, T. Kühl, A. N. Artemyev, and V. A. Yerokhin, *Phys. Rev. A* **56**, 252 (1997).
- [33] V. M. Shabaev, *Phys. Rep.* **356**, 119 (2002).
- [34] E. Arimondo, M. Inguscio, and P. Violino, *Rev. Mod. Phys.* **49**, 31 (1977).
- [35] G. Yang, J. Wang, B. Yang, and J. Wang, *Laser Phys. Lett.* **13**, 085702 (2016).
- [36] P. Fendel, S. D. Bergeson, Th. Udem, and T. W. Hänsch, *Opt. Lett.* **32**, 701 (2007).
- [37] J. E. Sansonetti, *J. Phys. Chem. Ref. Data* **36**, 497 (2007).
- [38] J. E. Simsarian, W. Z. Zhao, L. A. Orozco, and G. D. Sprouse, *Phys. Rev. A* **59**, 195 (1999).
- [39] A new value for the nuclear magnetic moment of  $^{210}\text{Fr}$  was determined in the work [17]. With this value, the agreement with experiment is excellent. However, this value actually corresponds to  $\mu(1 + \alpha/\pi F^{\text{QED}} +$

$\alpha/\pi F^{\text{BW}} - \alpha/\pi F^{\text{BW}'})$ , where  $F^{\text{QED}}$  and  $F^{\text{BW}}$  are semi-

empirically determined and  $F^{\text{BW}'}$  corresponds to the assumed magnetization distribution.